



Prometheusplein 1
Postbus 98
2600 MG DELFT
Telefoon: 015 - 2784636
Fax: 015 - 2785673
Email: Klanten-Service@Library.TUdelft.NL

Datum: 07-apr-03

Bonnummer: 648367

Aan: VLAAMS INSTITUUT VOOR DE ZEE
VISMIJN
PAKHUIZEN 45-52
B 8400 OOSTENDE
BELGIE

Tav:

Aantal kopieën: 9

Uw referentie(s): 1521555 1521555

Artikelomschrijving bij aanvraagnummer: 648367

Artikel: 3-D Shoreline Extraction from IKONOS Satellite Imagery

Auteur: Ron Li et al.

Tijdschrift: MARINE GEODESY

Jaar: 2003 **Vol.** 26

Aflevering: 1/2

Pagina(s): 107-115

Plaatsnr.: GEPR

Met ingang van 1 april 2003 zullen de prijzen voor fotokopie levering buitenland stijgen met € 0,05 per pagina

From April 1 2003, prices for photocopy delivery abroad will increase by € 0.05 per page

3-D Shoreline Extraction from IKONOS Satellite Imagery

RON LI
KAICHANG DI
RUIJIN MA

Department of Civil and Environmental Engineering and Geodetic Science
The Ohio State University
Columbus, Ohio, USA

Shorelines are recognized as unique features on Earth. They have valuable properties for a diverse user community. At present, photogrammetry is the most popular technique used to capture a shoreline. With improved resolution and accuracy, commercial high-resolution satellite imagery is demonstrating a great potential in the photogrammetry application domain. One example is the utilization of IKONOS satellite imagery in shoreline extraction. IKONOS panchromatic imagery has a resolution of approximately one meter as well as the capabilities of stereo imaging. This article presents the results of an experiment in which we attempted to improve IKONOS Rational Functions (RF) for a better ground accuracy and to employ the improved RF for 3-D shoreline extraction using 1-meter panchromatic stereo images in a Lake Erie coastal area. Two approaches were investigated. One was to rectify the ground coordinates derived from vendor-provided RF coefficients using ground control points (GCPs). The other was to refine the RF coefficients using the GCPs. We compare the results from these two approaches. An assessment of the shoreline extracted from IKONOS images compared with the existing shoreline is also conducted to demonstrate the potential of the IKONOS imagery for shoreline mapping.

Keywords shoreline, RF, aerial triangulation

Shorelines are recognized as unique features on Earth. They are one of 27 global “Geo-Indicators” referred to by the International Union of Geological Science (Lockwood 1997). Shoreline mapping has a history that began in 1807. Traditional shoreline mapping in small areas is carried out using conventional field surveying methods (Ingham 1992). Currently, the method most frequently employed for national shoreline mapping is photogrammetry. Recent developments in Global Positioning System (GPS) technology have stimulated an interest in its application to large-scale shoreline mapping. Land vehicle-based mobile mapping technology uses GPS receivers and a beach vehicle to trace water marks along a shoreline (Li 1997; Shaw and Allen 1995). LIDAR (Light Direction and Ranging) depth data have also been used to map regional and national shorelines (Ingham 1992).

Received 20 March 2002; accepted 20 June 2002.

This research was performed at The Ohio State University GIS & Mapping Laboratory. It was supported by a National Science Foundation Digital Government Grant and a grant from the National Sea Grant Program. Collaboration of the National Geodetic Survey, Coastal Services Center, and Office of Coastal Survey of the National Oceanic and Atmospheric Administration and the Ohio Department of Natural Resources is greatly appreciated.

Address correspondence to Ruijin Ma, Department of Civil and Environmental Engineering and Geodetic Science, The Ohio State University, Columbus, OH 43210-1275, USA. E-mail: li.282@osu.edu

With the launching of high-resolution satellites, a new era for digital mapping has opened, providing high-resolution images that can be utilized in shoreline mapping. IKONOS imagery from Space Imaging, Inc., is currently the only commercial high-resolution satellite imagery available to the public. Both 4-meter multispectral imagery and 1-meter panchromatic stereo imagery are available. With its capability for stereo imaging, it is hoped that IKONOS 1 m imagery can be used to replace the photogrammetry approach in some cases.

Rational Function (RF) is a model using a ratio of two polynomials to approximate the rigid imaging geometry. It executes the transformation between the object space and image space. For computational stability and to minimize computational errors, the image coordinates (x, y) and ground coordinates (X, Y, Z) are normalized to the range $[-1, 1]$ by their image size and geometric extent. Thus the RFs can be expressed as (Di et al. 2001; Madani 1999; OGC 1999; Whiteside 1997):

$$x = \frac{P_1(X, Y, Z)}{P_2(X, Y, Z)}, \quad y = \frac{P_3(X, Y, Z)}{P_4(X, Y, Z)}. \quad (1)$$

Polynomials P_i ($i = 1, 2, 3,$ and 4) have the general form:

$$P(X, Y, Z) = \sum_{i=0}^{m_1} \sum_{j=0}^{m_2} \sum_{k=0}^{m_3} a_{ijk} X^i Y^j Z^k. \quad (2)$$

In normal use, the order of the polynomials is limited to $0 \leq m_1 \leq 3$, $0 \leq m_2 \leq 3$, $0 \leq m_3 \leq 3$ and $m_1 + m_2 + m_3 \leq 3$. Each $P(X, Y, Z)$ is then a third-order, 20-term polynomial:

$$\begin{aligned} P(X, Y, Z) = & a_0 + a_1X + a_2Y + a_3Z + a_4X^2 + a_5XY + a_6XZ + a_7Y^2 \\ & + a_8YZ + a_9Z^2 + a_{10}X^3 + a_{11}X^2Y + a_{12}X^2Z + a_{13}XY^2 \\ & + a_{14}XYZ + a_{15}XZ^2 + a_{16}Y^3 + a_{17}Y^2Z + a_{18}YZ^2 + a_{19}Z^3. \end{aligned} \quad (3)$$

The RF coefficients in IKONOS products are calculated based on virtual control points generated from a rigorous sensor model. In cases where no GCPs are used, the RF coefficients provided may contain relatively large errors. Researchers have studied such errors and found that these errors often exist as systematic errors in linear form. In this article, we investigate a methodology for using IKONOS stereo imagery in digital shoreline mapping and for improving the ground point accuracy using two techniques developed for this research.

Accuracy Refinement for RF Outputs

The IKONOS images used in this experiment were taken in the Lake Erie coastal area in March 2001. In our project, we performed a GPS survey and obtained 11 control points. Image coordinates for these control points were measured manually. Ground coordinates were calculated using the Rational Function that came with the image data. After registering the two sets of ground coordinates within the same reference system, differences between these two control point sets were calculated (Figure 1). The display in Figure 1 is magnified 50 times for better visualization. From Figure 1, we can see that the dominant errors are

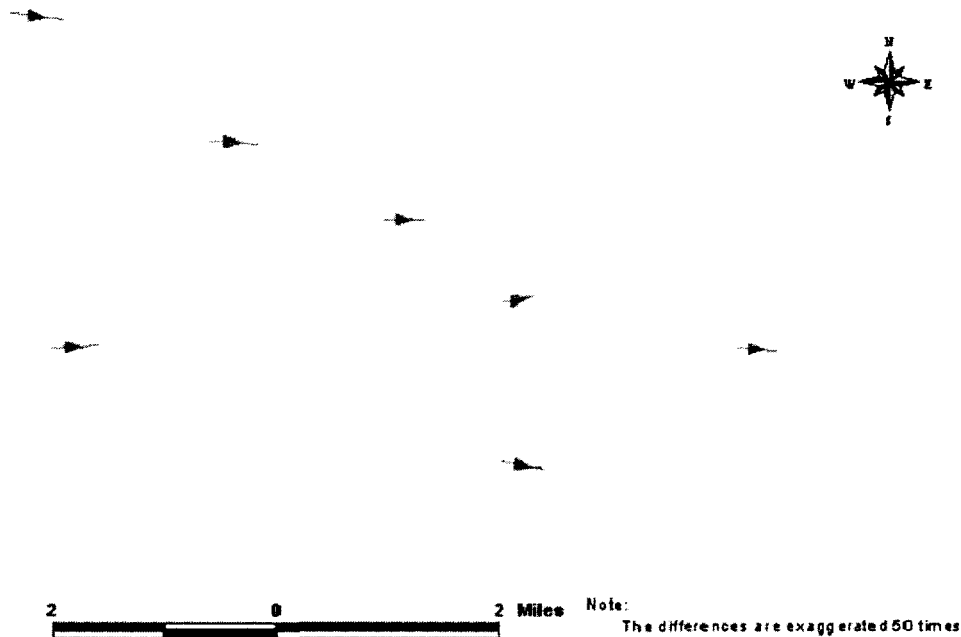


FIGURE 1 Systematic error distribution detected at GPS control points from IKONOS stereo images.

systematic and exist mainly in the X-direction. The maximum difference between GPS- and RF-derived coordinates for the control points falling within one stereo image pair equals 16 m. Thus the accuracy of the ground coordinates calculated from IKONOS RF should be improved if the satellite image data are to replace aerial photographs for shoreline extraction.

There are two ways to improve the accuracy of ground coordinates. As mentioned above, the RF model can approximate the rigid imaging geometry using vendor-provided RF coefficients. However, these coefficients are derived from virtual control points instead of ground truth. Thus the first approach is to improve the accuracy of the coordinates calculated from these rational functions by refining the vendor-provided RF coefficients based on ground truth. This method requires a large number of ground control points. The second approach is to directly refine the ground coordinates that were calculated from the vendor-provided RF. This second method is usually performed as a linear transformation based on significantly fewer ground control points than that used in the first approach. While the first method requires more control points, refinement is carried out at one time and the refined RF coefficients can be used in producing different products such as orthoimages and DEM. Though the second method requires fewer control points, the refinement process needs to be performed separately for each output. We investigated these two methods and discuss the results below.

Refinement of Vendor-Provided RF Coefficients (First Method)

An RF coefficient refinement method was developed based on the ground control points in order to increase the accuracy of the rational functions. New RF coefficients were calculated iteratively based on least-squares adjustments. In our research, derived RFs are in the same form as that of the vendor-provided RFs—the ratio of two third-order polynomials where the numerator and denominator in the rational functions are both third-order polynomials.

The functions we have are upward projection functions that transform ground coordinates into image coordinates. Considering the first coefficient in the denominator as a constant, there are in total 78 unknowns in both functions of X and Y coordinates. Thus at least 39 ground control points are needed for each image in the stereo pair. Unfortunately, there were less than 39 GPS control points available within the coverage area of the IKONOS images. To obtain sufficient high-accuracy control points for RF coefficient refinement, an aerial bundle adjustment of the NOAA/NGS aerial photographs was carried out and accurate orientation parameters of the aerial photographs were estimated.

In the bundle adjustment, 10 GPS control points were used. Tie points were intentionally selected so that they could also be picked up from the IKONOS image and thus, if sufficiently accurate, be used as control points in the RF coefficient refinement. After performing the bundle adjustment, we obtained 57 control points for each stereo image. These control points had accuracy levels of 0.3 m, 0.3 m, and 0.5 m, respectively, for the X, Y, and Z coordinates. We then refined the RF coefficients using these control points.

For each IKONOS image, 52 of the 57 GCPs were chosen to derive the new RF coefficients; the remaining five were used as checkpoints. Figure 2 shows the distribution of these points (Triangles are control points and dots are checkpoints).

The new RF were refined using a least-squares adjustment performed on the GCPs, taking the vendor-provided RF coefficients as the initial values to reduce the iterative computation. Ground coordinates of the checkpoints were computed by space intersections

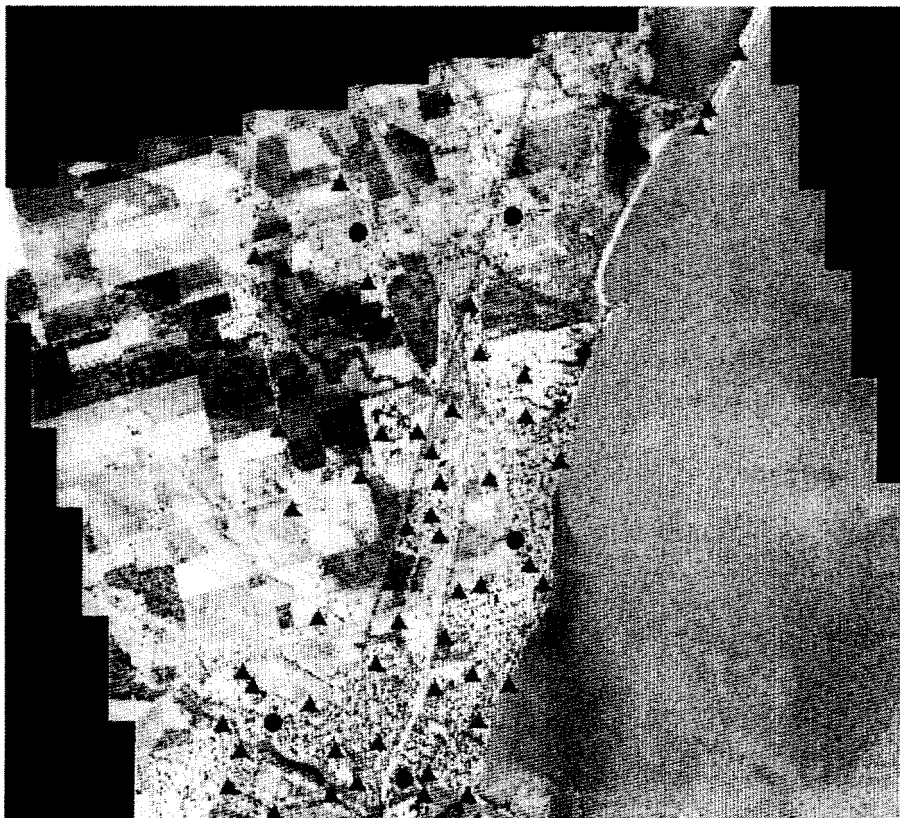


FIGURE 2 Distribution of control points (triangles) and checkpoints (dots) in the first stereo pair for RF coefficient refinement.

TABLE 1 RF Refinement Results

Refinement method	Stereo pair	RMS errors of the refined ground coordinates (m)		
		X	Y	Z
First method	Stereo 1	2.489	4.404	0.746
	Stereo 2	1.863	4.124	4.318
Second method	Stereo 1	1.342	1.051	1.632
	Stereo 2	0.991	0.787	1.513

using the refined RF coefficients. Accuracy of the refined RF coefficients was then assessed on the checkpoints by calculating the difference of their coordinates computed from the refined RF and the coordinates calculated from the aerial triangulation. Root Mean Square (RMS) differences are listed in Table 1.

It is important to note that horizontal ground coordinates calculated using the original and refined RF coefficients are in the geographic coordinate system in latitude (degree) and longitude (degree). The elevation unit is meters. All the measurements are in the WGS84 reference framework. Ground coordinates used in accuracy assessment were the coordinates in meters in a Universal Transverse Mercator (UTM) projection. This was done by transferring the geographic coordinates into UTM coordinates, after which the discrepancy was calculated.

Refinement of Ground Coordinates Calculated from Vendor-Provided RF (Second Method)

The second method is to correct the ground coordinates calculated from the vendor-provided rational functions directly using the ground control points. This method was tested using first-, second-, and third-order polynomials for a transformation from the RF-derived ground coordinates to the final corrected ground coordinates. Only the first-order polynomials were found to be most efficient. The other two have error levels of tens of meters. This is due to the fact that the errors between calculated and actual coordinates are linearly distributed. This experiment was also carried out on the ground control points. We first derived the transformation coefficients using the control points. Subsequently we transformed the checkpoints. By comparing the coordinates of the checkpoints calculated from the transformation with the coordinates calculated from the aerial photogrammetric triangulation, we obtained the RMS errors for the checkpoints. Nine GCPs and 45 checkpoints were used in Stereo Pair 1; eight GCPs and 49 checkpoints were used in Stereo Pair 2. See Figure 3 for the point distribution in the second stereo pair. Three of the 57 points in Stereo Pair 1 were eliminated because the discrepancies were too large and, therefore, they were treated as blunders. The RMS errors of the checkpoint ground coordinates for the Second Method are also listed in Table 1.

Comparing the results of these two refinement methods listed in Table 1, the second method (refining the ground coordinates from vendor-provided RF) appears superior. This outcome may be partly due to the result of the flatness of the test site (where a polynomial fit is more effective). Further research with mountainous terrain data sets may conclude differently. The over parameterization issue should also be investigated. In general, ground coordinates derived using either method can reach an accuracy of 2 to 4 meters.

The U.S. Geological Survey (USGS) 1:24,000 scale topographic map is accurate to approximately 12.2 meters. The National Oceanic and Atmospheric Administration/National

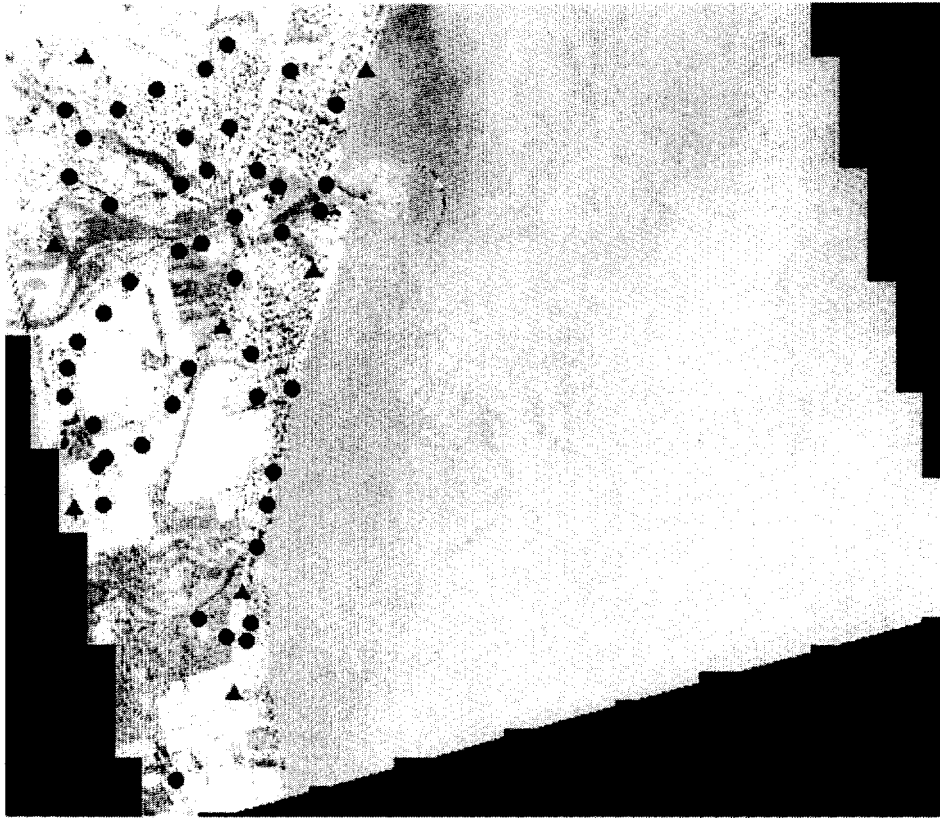


FIGURE 3 Control and check point distribution in the second stereo pair for coordinate refinement.

Geodetic Survey (NOAA/NGS) 1:5,000 scale Coastal Topographic Survey Sheet (T-Sheet) is accurate to approximately 2.5 meters (Li et al. 2001). In comparison, ground points derived from IKONOS 1-meter panchromatic stereo images reach an accuracy level close to the NOAA/NGS T-Sheets and are more accurate than the USGS 1:24,000 topographic maps. Thus IKONOS imagery in certain situations can achieve the same accuracy level as the photogrammetric approach for coastal mapping, while providing less expensive processing and production procedures in the future.

3-D Shoreline Extraction from IKONOS Imagery

Shoreline Extraction in Image Space

Deriving a shoreline from IKONOS images is done by calculating shoreline ground coordinates from shoreline image coordinates using rational functions. In this procedure, the first step is to obtain the shoreline image coordinates in both images of a stereo pair. During satellite imaging, one ground point is projected onto both images of the stereo pair. The resulting points in the stereo images are called conjugate points. The major task in shoreline calculation is to find the conjugate points on the shoreline in both images. We first attempted to pick up the conjugate points manually and then connected these points in a sequence to represent the shoreline. This work was very labor intensive. In addition, it is very difficult to find the conjugate point on the shoreline in areas where the shoreline does not have much

curvature change and the background does not have sufficient texture information. To solve these problems, we developed a semiautomatic method. A shoreline was digitized in one stereo image by manually selecting the shoreline vertices. Then the conjugate points of these vertices in the other stereo image were determined using an image-matching method.

The manually digitized shoreline was overlaid on the first image to make sure that sufficient digitized points are used to represent the shoreline in each image. Extraction of the conjugate points in the other image should be performed with great care because mismatched conjugate points can produce significant errors in the computed ground coordinates. The shoreline is a clear feature on the IKONOS stereo images that are resampled using epipolar geometry by the vendor so that y-parallax values of the conjugate points are very small (Grodecki 2001). In our data set, the maximum y-parallax is 3 pixels with most values being 0 or 1 pixel. Thus, an area-based matching using normalized correlation coefficients was performed directly in the original images. Figure 4 shows the matched points in the Sheldon Marsh area. There are 560 points matched along the shoreline. We used ArcView software to check the quality of the matched points and edit them. Six mismatched points were deleted and 12 points were added manually. For the second stereo pair, we manually selected 192 points in one image. Their conjugate points were all found by the area-based image matching technique.

3-D Shoreline Calculation

3-D coordinates of the shoreline can be calculated from the matched image points in the stereo images using upward rational functions (Di et al. 2001). Since the rational functions calculate the image coordinates from the ground coordinates, an iteration algorithm was employed. Note that the RF coefficients were refined by using the ground control points. A transformation was carried out to convert the geographic coordinates (latitude, longitude)

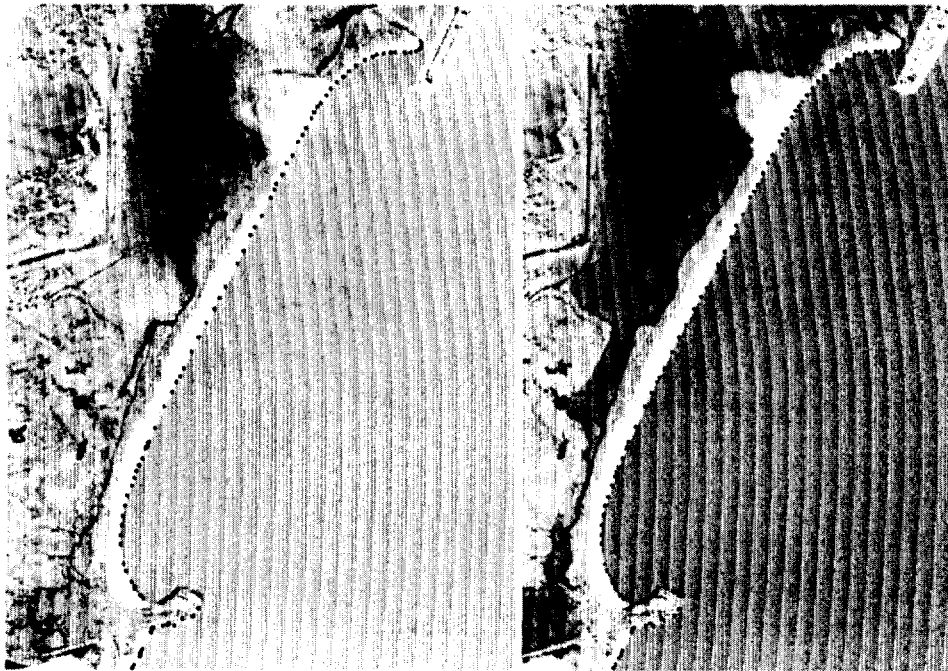


FIGURE 4 Matched shoreline points in first and second image.

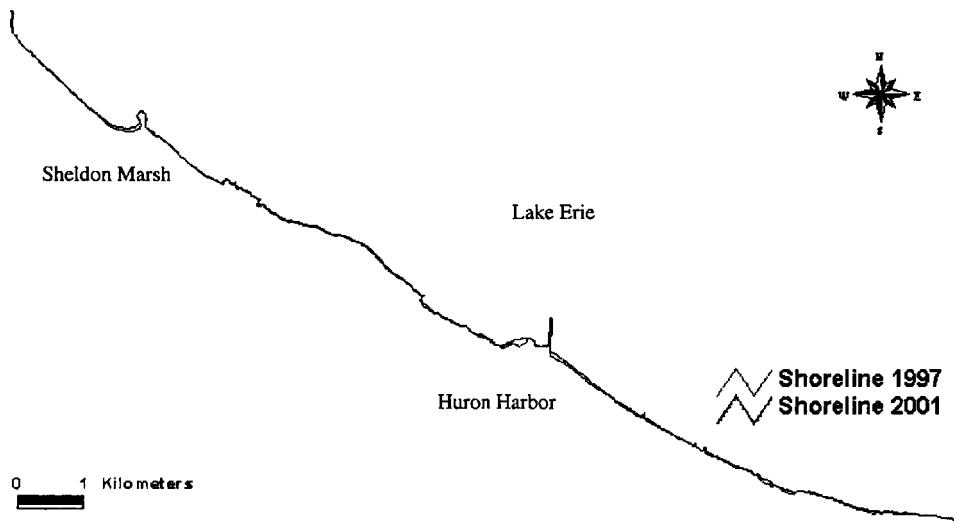


FIGURE 5 Shorelines from 1997 aerial photos and 2001 IKONOS imagery.

into the UTM coordinates (X, Y). Figure 5 shows the calculated shoreline from the IKONOS stereo images along with the shoreline extracted from 1997 orthophotographs generated from NOAA aerial images. Figure 6 illustrates both shorelines in an enlarged area of Sheldon Marsh. The solid line is the shoreline from the 1997 aerial orthophotographs and the spurred line is the shoreline calculated from the 2001 IKONOS stereo images.

In Figure 6, the difference between the two shorelines is obvious. The maximum difference is approximately 43 m (seen in the lower right section). We can also see that a

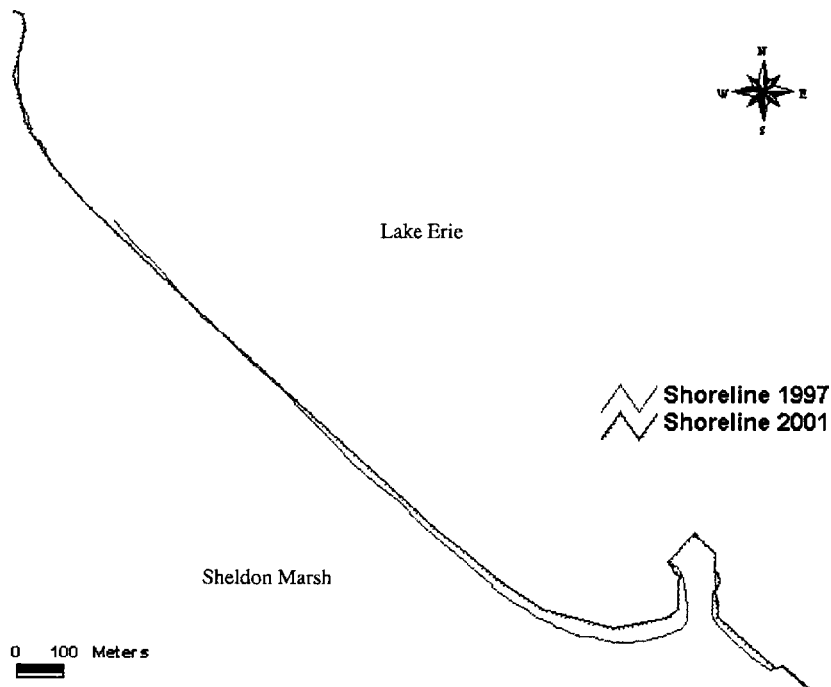


FIGURE 6 Shorelines enlarged from Figure 5 in Sheldon Marsh area.

portion of the 2001 shoreline extends into what was formerly the lake. This is because the water level in Lake Erie has dropped significantly in the past three years. In addition, the sand barriers were disconnected in 1997 and are now connected in 2001 when the water level dropped. There are also sections where the shoreline moved landwards, showing erosion.

Conclusion

Shoreline mapping is attracting increasing attention from experts of photogrammetry, remote sensing, and GIS. The new generation of commercial satellites offers high-resolution image data as well as the capability for stereo imaging. Thus they provide new possibilities for efficient shoreline mapping. This study demonstrates that a shoreline derived from IKONOS satellite imagery can reach a ground accuracy of about 2–4 meters, which is close to the NOAA/NGS 1:5,000 T-Sheet accuracy and higher than the accuracy of USGS 1:24,000 topography maps. Shorelines thus derived can be used in a variety of coastal applications.

The above shorelines are not tide-coordinated shorelines (Li et al. 2002) referenced to MLLWL (Mean Lower-low Water Level) or MHWL (Mean High Water Level). Derivation of such tide-coordinated shorelines from the instantaneous shorelines from IKONOS imagery is a subject of our current research.

References

- Di, K., R. Ma, and R. Li. 2001. Deriving 3-D shorelines from high resolution IKONOS satellite images with rational functions. *Proceedings of ASPRS Annual Convention*, St. Louis, MO, April 25–27, 2001, (CD-ROM).
- Grodecki, J. 2001. IKONOS stereo feature extraction—RPC approach. *Proceedings of ASPRS Annual Convention*, St. Louis, MO, April 25–27, 2001, (CD-ROM).
- Ingham, A. E. 1992. *Hydrography for Surveyors and Engineers*, p. 132. London: Blackwell Scientific Publications.
- Li, R. 1997. Mobile mapping: An emerging technology for spatial data acquisition. *Photogrammetric Engineering & Remote Sensing* 63(9):1165–1169.
- Li, R., K. Di, G. Zhou, R. Ma, T. Ali, and Y. Felus. 2001. Coastline mapping and change detection using one-meter resolution satellite imagery. Project Report submitted to Sea Grant/NOAA, 146 pp.
- Li, R., R. Ma, and K. Di. 2002. Digital tide-coordinated shoreline. *J. Marine Geodesy* 25(1/2), 27–36.
- Lockwood, M. 1997. NSDI Shoreline briefing to the FGDC coordination group, NOAA/NOS. Washington, DC.
- Madani, M. 1999. Real-time sensor-independent positioning by rational functions. *Proceedings of ISPRS Workshop on Direct Versus Indirect Methods of Sensor Orientation*, Barcelona, Nov. 25–26, 1999, pp. 64–75.
- Open GIS Consortium. 1999. The OpenGIS™ abstract specification, Topic 7: The earth imagery case. URL: <http://www.opengis.org/public/abstract/99-107.pdf>
- Shaw, B., and J. R. Allen. 1995. Analysis of a dynamic shoreline at Sandy Hook, New Jersey, using a geographic information system. *Proceedings of ASPRS/ACSM, 1995*, pp. 382–391.
- Whiteside, A. 1997. Recommended standard image geometry models, Open GIS Consortium. URL: <http://www.opengis.org/ipt/9702tf/UniversalImage/TaskForc.ppt>